ACI MATERIALS JOURNAL
A JOURNAL OF THE AMERICAN CONCRETE INSTITUTE

Experimental Investigation of Blast-Pressure Attenuation by Cellular Concrete

Weimin Nian, Kolluru V. L. Subramaniam*, and Yiannis Andreopoulos

* Department of Civil Engineering , Indian Institute of Technology (IIT) Hyderabad, Ordnance Factory Estate Campus , Yeddumailaram , India

Materials Journal
Volume 112, Issue 1, 2015, Pages 21-28
http://dx.doi.org/10.14359/51687242

Experimental Investigation of Blast Pressure Attenuation by Cellular Concrete

Weimin Nian, Kolluru V.L. Subramaniam, and Yiannis Andreopoulos

Weimin Nian is Structural Engineer at Engineering Group Associates. He received his PhD from the City College of New York

Kolluru V.L. Subramaniam is a Professor and the Head of the Department of Civil Engineering at Indian Institute of Technology Hyderabad. He obtained his B.Tech. degree from Indian Institute of Technology Delhi and PhD from Northwestern University. He is a

Fellow of ACI and a member of ACI committees 215 (Fatigue), 123 (Research) and 446 (Fracture).

Yiannis Anderopoulos is the Michael Pope Professor of Energy Research in the Department of Mechanical Engineering at the City College of New York. He received his PhD from the Imperial College, London University.

ABSTRACT

Results from an experimental investigation of the dynamic response of cellular concrete subjected to blast pressure loading are presented. The cellular structure consisted of large entrained porosity in the form of uniformly distributed air cells in a matrix of hardened cement. Under quasi-static loading, once the applied stress exceeds the crushing strength of the cellular concrete, crushing and densification of material results in an upward concave stress-strain response. The shock-tube experimental test setup used for generating blast pressure loading in a controlled manner is described. Experimental results from the cellular concrete subjected to blast pressure loading with pressure amplitude greater than the crushing strength of foam indicate that a compression stress wave, which produces compaction of the material due to collapse of the cellular structure, is produced in the material. As the compaction front propagates in the material, there is a continuous decrease in its amplitude. The impulse of the blast pressure wave is conserved. When sufficient length of the cellular concrete is present, the applied blast pressure wave is completely attenuated to a rectangular stress pulse. The transmitted stress to a substrate from cellular concrete when an applied blast pressure wave is completely attenuated resembles a

rectangular stress pulse of amplitude slightly higher than the crushing strength of the material with a duration predicted by the applied blast impulse.

Keywords: Blast, cellular concrete, crushing, dissipation, protection, shock, impact, impulse

INTRODUCTION

A blast pressure wave consists of a compression shock front followed by a rarefaction (expansion) wave as shown in Figure 1 [1-2]. The duration of the shock and the compression wave are typically in the order of micro-seconds (10^{-6} s). The entire blast pressure wave lasts up to few milli seconds (10^{-3} s). Developing blast retrofit measures primarily focuses on dealing with the pressure wave and its effects on structural elements. There are several time-scales in the blast response of the structural element as shown in Figure 1. In the very short time scale (on the order of duration of the compression wave), the transient response is governed by the stress changes produced by wave propagation in the material. With time, the response evolves to produce vibration of the entire structural element at frequencies which are determined by the stiffness of the element and the boundary conditions [2-6]. The motion of the structural element associated with the vibration response occurs in the milli-second time-scale. The vibration response might be completely absent in the case where complete failure or loss of integrity is produced by the propagating wave in the material. In the short time scales, a large magnitude blast can result in significant damage and even brittle shattering in concrete or masonry leading to a collapse of the structural element [3,4,6,7]. The failure of a few critical load-bearing

structural elements may eventually lead to the progressive collapse of the entire structure [8].

Most of the blast mitigation strategies for existing buildings and structures that are currently in practice, fall in the category of structural strengthening and/or restraint systems, which enhance the strength, stiffness and continuity in critical elements. Blast retrofit measures based on strengthening a structural element are only effective in the time scale associated with the vibration motion of the structural element (typically in the order of milli-seconds). Strengthening measures do not directly influence the magnitude of the stress wave generated in the material when the blast wave is incident on the structural element. Stress changes in the material due to wave propagation occur on the time scale which is of the order of micro-seconds (three orders of magnitude smaller than the time scale associated with vibration or structural motion). In the case of quasi-brittle materials, such as masonry and concrete, the stress wave induced by the blast pressure loading may cause severe material damage in the form of crushing, cracking or spalling, before there is any noticeable displacement of the structural element [9]. There is hence a need to develop protective systems for structural elements, which decrease the amplitude of the blast pressure experienced by the material of the structural element. Such protective systems can then be used in conjunction with strengthening systems for developing effective blast mitigation strategies, which are effective at both time scales associated with the blast response of a structural element.

Cellular materials possess energy-absorbing properties and are widely used as

protective materials in applications such as, improving crash worthiness [10, 11]. Successful use of these materials in mitigating impacts has drawn the attention of structural community towards the development of blast mitigation strategies. Material systems based on cellular concrete are suited for developing applications which require energy dissipation. A porous, low-strength cementitious material,[1] with low impedance (resistance) to shock wave propagation will undergo irreversible compaction. This damage mechanism in the porous material results in energy dissipation and hence produces attenuation of the stress wave. A sacrificial cladding made of cellular concrete is intended for use as protective measure, which would reduce the stress amplitude transmitted to the structural element from an applied blast pressure loading.

In this paper, the results of an experimental investigation of the dynamic response of cellular concretes subjected to blast pressure loading are presented. Controlled blast pressure loading with different amplitudes and varying durations were generated using a shock tube. For an applied blast pressure loading, the stress transmitted to an elastic substrate through cellular concrete of different densities and different lengths were evaluated. The deformation of the cellular concrete bars after application of the blast pressure loading was recorded. It is shown that crushing of the cellular concrete results in a decrease in the transmitted stress amplitude.

RESEARCH SIGNIFICANCE

[1]Porous cementitious material implies a material with a cementitious matrix which contains entrained porosity. Entrained porosity is introduced by the addition of air bubbles or other low strength inclusions.

Blast vulnerability of buildings in an urban environment has motivated the Structural Engineering community to develop and implement blast mitigation strategies for existing structures. Studies have shown that in densely constructed space, buildings which are not the primary target will also be subjected to intense pressure loading not originally designed for. One of the objectives of developing blast retrofit measures, primarily focuses on dealing with the pressure wave and its effects on buildings.

Protective material systems which use porous metal foams for attenuating an incoming blast wave are being researched for specialized applications such as protection of armaments and armor systems [11 - 13]. The use of aluminium foam to mitigate blast loading has also been evaluated through full-scale explosion tests [13]. Applications based on metal foams are however impractical for infrastructure applications because of cost concerns. Besides economic considerations, typical aluminium foam samples cannot be cast readily or produced using simple techniques which would be adapted to the field. Use of protective cladding made of cellular concrete as a sacrificial protective material, which would reduce the stress amplitude transmitted to the structural element from an applied blast pressure loading offers a practical solution, which can be produced in the large quantity required for a typical infrastructure application using readily available technology.

The use of cellular concrete for providing energy dissipation in impact and blast applications in buried structures has been proposed before [14]. Results of impact studies showed that cellular concrete can accommodate projectiles and fragments by predominantly plastic failure. A commercial product, SACON^{TM}, which uses low strength

concrete as bullet and shock absorbing material has been developed for use in bullet and fragment absorbing concrete, backstops and blast protection walls.

Studies have shown that low density concrete can be used in buried protective structures for absorbing ground motion, dissipating shock energy and transmit particular design stress level to the structure. The use of low strength concretes for protection of buried structures as a backpacking material has also been considered [15]. Besides economic considerations, the use of low density concrete for developing blast and impact protection of structures and silos was shown to be attractive considering the ease of handling, placing and production [14].

Brittle shattering or spalling of structural elements, primarily made of reinforced concrete or brick masonry, can be prevented or suppressed in structural elements with a cladding of cellular concrete. Analysis of the beneficial effect of cellular concrete is usually performed using assumed material behaviour of cellular concrete [14, 15]. Experimental data on the blast response of cellular concrete is very limited. Such information would be very beneficial in developing better predictive approaches and for designing cladding for blast mitigation.

OBJECTIVES

The objectives of this work are:

1. To investigate the response of cellular concrete subjected to blast pressure loading.

2. To determine the transmitted stress amplitude and history as a function of crushing strength of cellular concrete.

EXPERIMENTAL TEST SETUP

A shock-tube was used for generating blast pressure waves with the required amplitude and duration. A schematic sketch and a photograph of the test facility are shown in Figure 2. The shock tube consisted of a high pressure section (driver section) which was separated from a low pressure section (driven section) by a diaphragm. Pressure ports were machined at different locations along the length of the driven section for mounting pressure transducers. Pressure transducers were placed flush with the inner surface of the tube. The driven section of diameter 4.5 cm (1.77 in) was connected to the driver section with diameter equal to 8.9 cm (3.50 in) using a 20 cm (7.9 in) long nozzle. The diameter decreased smoothly from 8.9 cm (3.5 in) to 4.5 cm (1.77 in) over the length of nozzle. The nozzle was used to accelerate and increase the Mach number of the flow. During the test, the sample made of cellular concrete was attached in front of an instrumented steel rod and subjected to blast pressure loading. The instrumented rod was used to measure the transmitted stress from the cellular concrete.

The pressure wave was generated by the rupture of a diaphragm which was pressurized on one of its faces. Gas of high pressure was filled in the driver section and the gas pressure was increased until the diaphragm ruptured. Diaphragm made of Aluminium 6061-T6 was used. Two perpendicular notches were machined on one of the faces of the diaphragm to ensure that it opened completely upon rupture. The thickness of the

diaphragm was equal to 1.6 mm (0.063 in) and notches with different depths ranging from 0.8 mm (0.03 in) to 1 mm (0.04 in) were machined to obtain blast pressure waves with different amplitudes.

Pressure loading produced by the blast wave was measured using pressure transducers, placed close to the target end in the driver section of the shock tube. A typical blast pressure history is shown in Figure 2(c). The reflected pressure history clearly shows an exponential decay in pressure (the exponential decay function fit to the data is shown in the figure by the dashed line). The reflected blast pressure amplitude decreased to 10% of the peak reflected blast pressure amplitude within 5 ms. Different blast loads with pressure amplitudes ranging from 0.5 MPa (72.5 psi) to 1.5 MPa (217.5 psi) and duration in the order of several ms were generated.

MATERIALS AND METHODS

Cellular concretes consisting of large entrained porosity in the form of uniformly distributed air cells were used in the study. The air cells were introduced by mixing a stable, voluminous, micro-bubbled foam into cement paste. The porosity of the mix was varied by controlling the volume of foam mixed into the cement paste. After setting, when the cement paste gained strength, the cementitious matrix developed a cellular structure. The bubbles in the foam formed a disconnected pore space.

Cellular concretes used in this study were made using cement paste with a water to cement ratio (by weight) equal to 0.55. The cement paste was prepared by mixing cement

and water in a paddle mixer. Polypropylene fibers (Stealth® e3 micro-reinforcement, classification D700/800) were also added to the cement paste. Approximately, 10 grams (0.35 ounces) of fibers were used for each 5 kg (11 lb) of cement paste. The foam was generated using a foam generator. A commercially available foaming agent, MEARLCRETE®, which is an aqueous concentrate of a surface-active Polypeptide-Alkylene Polyol condensate, specially formulated to yield tough, stable, voluminous micro bubbled foam was used. The foaming agent was diluted in water at the recommended dosage and mixed with air in the foam generator. The foam was then hand mixed with the cement paste and cement foams with two different wet cast densities equal to 432 kg/m^3 (27 lb/ft^3) and 528 kg/m^3 (33 lb/ft^3) were produced by varying the volume of foam added to the cement paste. Cylindrical samples with diameter equal to 44 mm were prepared using acrylic molds. The inner surface of the mold was lined with a Teflon paper. The paste with the entrained foam was poured into the mold in layers and gently tapped on the sides to ensure proper placement. After 7 days, the cellular concrete samples were demolded and left to dry in the laboratory environment (maintained at 23 ^oC (73.4 ^oF) and 50% RH). The dry densities of the cellular concrete after 7 days were equal to 384 kg/m^3 (24 lb/ft^3) and 480 kg/m^3 (30 lb/ft^3).

A photograph of the cellular microstructure of a typical cellular concrete sample showing the dispersion of air cells is shown in Figure 3. Confined compression tests were performed 28 days after casting to obtain the quasi-static load response. The cellular concrete samples were placed inside an acrylic tube with inner and outer diameters equal to 44.5 mm (1.75 in) and 50.8 mm (2.0 in), respectively. Confined compression tests were

performed to provide a basis for comparison with the blast response obtained in the shock tube where the lateral expansion of the cellular concrete is constrained. To minimize the influence of friction on the test response the cellular concrete was wrapped with two sheets of Teflon and a low viscosity oil was placed in the gap between the Teflon sheet and the inner wall of the acrylic tube. Load was applied to the cellular concrete sample using a steel cylinder which slid smoothly inside the acrylic tube. The total deformation of cellular concrete was measured and engineering strain was computed as the relative displacement between the two ends of the cellular concrete divided by the original length of the cellular concrete.

Typical quasi static load response of the cellular concrete is shown in Figure 4. In the initial linear elastic region the material follows Hooke's law. Following the linear response the stress-strain curve exhibits an upward concave shape. The abrupt change in the slope of the stress-strain response at the end of the linear response is due to initiation of crushing within the cells. The stress at the end of the linear response is also known as the crushing strength of cellular concrete. The concave response which follows is associated with the collapse of the internal structure and densification of the material. The cell collapse is associated with brittle crushing of the cell walls [11 pp. 203]. In the concave part of the load response, upon unloading there is significant permanent shortening associated with compaction of the material due to crushing of cells. It should be noted that while engineering strain is calculated using the overall shortening of the entire length of cellular concrete, the local deformation in the material is non-uniform in the concave part of the load-envelope.

Static stress-strain curves of cellular concretes were fitted using the function give in Equation 1 with the parameters given in Table 1.

$$\sigma = \begin{cases} E\varepsilon & \varepsilon \le \varepsilon_{po} \\ \sigma_{po} - AE\left(1-\varepsilon_{po}\right)^{\alpha} + AE\left(1-\varepsilon\right)^{-\alpha} & \varepsilon > \varepsilon_{po} \end{cases} \quad (1)$$

where ε is the engineering strain, α is a constant greater than zero, A and E are material constants, ε_{po} and σ_{po} ($=\varepsilon_{po} \times E$) are the strain and stress associated with crushing strength of cellular concrete. The average crushing strength of cellular concrete with dry densities equal to 384 kg/m^3 (24 lb/ft^3) and 480 kg/m^3 (30 lb/ft^3) were equal to 0.384 MPa (55.7 psi) and 0.63 MPa (91.3 psi), respectively. As expected there is an increase in the crushing strength with an increase in density of the material.

EXPERIMENTAL RESULTS

To study the effect of cellular concrete in mitigating different blast loads, cellular concrete samples were tested using blast pressure loads with different pressure amplitudes. Cellular concrete specimens of length, L = 230 mm (9 in), and 190 mm (7.5 in) were used for cellular concrete of dry density 384 kg/m^3 (24 lb/ft^3) and for the cellular concrete with dry density equal to 480 kg/m^3 (30 lb/ft^3), the length of the cellular concrete specimens was equal to 180 mm (7.1 in) and 115 mm (4.52 in). The cellular concrete specimens were subjected to blast loadings with two different amplitudes. The amplitudes of the high level blasts were greater than or equal to 1.2 MPa (188.5 psi) while the amplitude of the low level blast was lower than 1.0 MPa (145 psi) but higher than 0.8 MPa (116 psi). Samples of length 230 mm (9 in) and 180 mm (7.1 in) were tested under high level blast loads for

cellular concrete with dry density equal to 384 kg/m^3 (24 lb/ft^3) and 480 kg/m^3 (30 lb/ft^3), respectively. Samples of length 190 mm (7.5 in) and 115 mm (4.52 in) were tested under low level blast loads for cellular concrete with dry density equal to 384 kg/m^3 (24 lb/ft^3) and 480 kg/m^3 (30 lb/ft^3), respectively.

The applied blast pressure and transmitted stress histories are shown in Figure 5. The rupture of the membrane was used to trigger the data collection. The blast pressure was measured using a pressure transducer placed at a small distance from the face of the sample. The actual distance depends upon the length of the sample. The initial rise in pressure signals the passage of the initial blast pressure wave created by the rupture of the membrane. This is followed by a larger increase in pressure, which is the reflected pressure from the cellular concrete sample. The reflected pressure history at the face of the cellular concrete sample is representative of the applied pressure history.

The transmitted stress history measured using the instrumented steel rod is shown in Figure 5. There is time lag between the reflected pressure and the measured transmitted stress. This corresponds to the time taken by the stress pulse to propagate through the cellular concrete. The transmitted stress shows a predominantly rectangular profile with an abrupt rise followed by an essentially constant stress. After the initial plateau, the transmitted stress exhibits a sudden drop followed by a decreasing profile similar to the applied stress history. The amplitudes of the rectangular pulses are nominally higher, but close to the crushing strengths of the cellular concrete regardless of the applied blast pressure amplitude (σ_{po}=0.384 MPa (55.7 psi) for 384 kg/m^3 (24 lb/ft^3) cement form and

σ_{po} = 0.63 MPa (91.3 psi) for 480 kg/m^3 (30 lb/ft^3) cement form). The duration of the transmitted rectangular pulse, on the other hand, increases with an increase in the applied blast pressure amplitude.

Typical photographs of a cellular concrete sample with density equal to 384 kg/m^3 before and after testing are shown in Figure 6. A ruler with major divisions equal to 12.7 mm (0.5 in) and minor divisions at 6.35 mm (0.25 in) was marked on the specimen prior to application of blast pressure loading. A ruler is placed next to the specimen for reference. In addition, lines of equal spacing coinciding with initial grid are also drawn on the photograph of the specimen obtained after testing. It can clearly be seen that the cellular concrete is irreversibly compacted after blast pressure loading. Closer inspection reveals that cellular concrete up to the first five divisions at the front end is irreversibly compacted, while the middle portion of the cellular concrete (between divisions 5 and 9) is relatively intact. Some crushing and irreversible damage is also observed in the last five divisions. The extent of compaction is higher on the front loaded end than on the back end; the spacing of markings after compaction is closer on the front end than on the back end.

The observed experimental response can be explained considering propagation of the stress wave through the cellular concrete [17]. The applied blast pressure amplitude produces an increase in stress at the loaded end beyond the crushing strength of the foam. Stress wave(s) of different magnitudes are produced in the cellular concrete. An elastic wave which propagates at a speed predicted by the initial elastic modulus of the material travels into the material. Since the initial applied pressure amplitude is higher than the

crushing strength of the cellular concrete, it produces compaction of the cellular concrete. Two waves are thus formed in the material: (a) A faster elastic stress wave with amplitude equal to the crushing strength of cellular concrete; and (b). A slower compaction front, which produces densification of material in its wake. The elastic wave travels with constant amplitude as it propagates in the material. The compaction front continuously decreases in amplitude as it propagates into the material due to energy dissipation provided by compaction of the material. When the amplitude of the compaction front decreases to a value equal to the crushing strength of the cellular concrete, compaction of the material stops. The elastic wave continues to propagate in the material and when it reaches the back end, reflection produces wave(s) travelling in the backward direction. There is an increase in the stress upon reflection from a substrate of higher stiffness; the stress increases above the crushing strength of foam. The stress transmitted to the substrate, which corresponds to the amplitude of the reflected pressure is therefore higher than the crushing strength of the foam. An elastic wave and a compaction front travelling in the reverse direction are produced after reflection. The compaction front produces densification till attenuation produced by compaction reduces its amplitude to the crushing strength of cellular concrete. The stress waves produced in the foam therefore produce compaction at both the front and the back ends of the foam.

ANALYSIS OF RESULTS

The results from the transmitted stress history indicate that the impulse transferred to the solid substrate is not affected by the presence of cellular concrete. The impulse is the time integration of the corresponding pressure/stress curves in Figure 5. The impulse

corresponding to the applied pressure and transmitted stress histories for the cellular concrete with crushing strength equal to 0.384 MPa (55.7 psi) are shown in Figure 7. The applied impulse was calculated from the reflected pressure history. Figure 7 clearly shows that the impulse of transmitted stress is equal to the applied impulse at the end of the loading history. This suggests that the impulse is conserved despite the irreversible compaction and energy dissipation in the cellular concrete.

In a material which exhibits concave stress-strain response, the existence of the minimum length of material to attenuate the initial compaction front has previously been predicted using simplified a rigid-perfectly-plastic-locking (RPPL) idealization of the actual stress-strain response [16-19]. In the RRPL idealization, the crushing and densification of the material occurs at a constant value of stress up to a fixed value of strain, following which the material exhibits a rigid behavior. The RPPL idealization for the cellular concrete is shown in Figure 4. The minimum length of the cellular concrete required to completely attenuate the applied blast pressure wave as it propagates down the length of the material, which is equal to the length of compacted foam on the front end, depends upon the impulse of the blast pressure wave and the crushing strength of the foam. The length of the cellular foam increases with an increase in the applied blast pressure impulse and decreases with the increase in the crushing strength of the material. The theoretical calculation shows that compaction ends when the impulse of the applied blast pressure wave equals the impulse of the transmitted stress wave with amplitude equal to the crushing strength of the material [19]. The experimental results indicate that the impulse of the applied blast pressure wave is conserved. The transmitted stress wave in the

instrumented steel rod at the back end has the same impulse as the applied blast pressure loading.

Reflection at the back end, which occurs at the interface between the cellular concrete and instrumented steel rod results in a stress amplification. The stress wave produced by reflection at the back end has an amplitude, which is slightly higher than the crushing strength (as indicated by the measured transmitted stress). The reflected stress wave which travels in the reverse direction produces compaction of foam. Therefore a length of foam is also compacted at the back end until the stress amplitude decreases to the crushing strength of foam. However, since the amplitude of the reflected stress wave is only slightly higher than the crushing strength, the level of compaction is smaller at the back end. Experimental evidence confirms that while the cellular concrete sample is compacted at both ends, the extent of compaction is higher at the front end when compared to the back end, as seen in Figure 6.

Results indicate that the stress wave in the cellular concrete is attenuated to an amplitude equal to its crushing strength. Since the impulse of the applied blast pressure loading is conserved, the duration of the rectangular stress wave in the cellular material depends on the applied blast impulse. For a given blast pressure loading, the length of cellular concrete required to attenuate the applied pressure amplitude to crushing strength should equal the lengths required at both the front and back ends. It is possible that the length of cellular concrete is insufficient to attenuate the applied blast pressure wave. In this case the transmitted stress to the substrate will increase significantly higher than the

crushing strength of cellular concrete. There is thus a certain minimum length of cellular concrete which is required to completely attenuate the applied blast pressure wave. If the length exceeds the required minimum some length of the cellular concrete will remain uncompacted, as seen in the results presented here.

For using cellular concrete as protective cladding in blast applications, the minimum length required should consider compaction at both the front and back ends. If the length of cellular concrete is larger than the sum of the minimum lengths required for attenuating the compaction fronts at the front and back ends, the transmitted stress to the substrate can be reduced to a magnitude which is nominally higher than the crushing strength of the material. Therefore, for a blast of a given impulse, cellular concrete can be used to control the stress transferred to the concrete structure by using material with different crushing strength.

CONCLUSIONS

There is clearly a beneficial effect of reduction in the stress amplitude achieved by placing cellular concrete in the path of a blast pressure wave. The applied blast pressure wave with pressure amplitude greater than the crushing strength of the cellular concrete produces irreversible compaction in the cellular concrete, which produces attenuation of the stress. The crushing of the cellular concrete produces a change in the stress profile of the transmitted stress pulse when compared with the applied blast pressure wave. There is a minimum length of cellular concrete which will ensure complete attenuation of the applied pressure wave. When the minimum length is exceeded, the blast load applied at the

loaded end of the cellular concrete bar is transferred as a rectangular shaped stress pulse at the target end. The magnitude of the transferred stress is nominally higher than the crushing strength of cellular concrete. There is no change in the impulse of the transmitted stress pulse when compared with the applied blast pressure wave.

REFERENCES

1. Kingery, C.N., and Bulmash, G., (1988), "Air-blast Parameters from TNT Spherical Air Burst and Hemi-spherical Surface Burst," Technical Report ARBRL-TR-02555, US Army Armament Research Development Center, Ballistic Research Laboratory, Aberdeen Proving Ground, Maryland.
2. US Department of the Army, (1990), "Structures to resist the effects of accidental explosions," Technical manual TM5-1300, Washington, DC
3. Conley, C.H. and Gregory, F.H., (2000), "Modeling of Blast-Loaded Structural Panels," Proceedings of the 8th Annual U.S. Army Research Laboratory/ United States Military Academy Technical Symposium, Sponsored by The Mathematical Sciences Center of Excellence, West Point, NY, pp. 221-235, November 3.
4. Conley, C.H., and Gregory, F.H., (1999), "Vulnerability of Structural Panels to Blast Effects," proceedings of the 70th Shock & Vibration Symposium, Albuquerque, NM, November 15-19.
5. Mosalam, K. M., and Mosallam, A.S., (2001), "Nonlinear Transient Analysis of Reinforced Concrete Slabs Subjected to Blast Loading and Retrofitted with CFRP Composites," *Composites, Part B: Engineering*, No. 32, pp. 623-636.

6. Davidson, J.S., Fisher, J.W., Hammons, M.I., Porter, J.R., and Dinan, R.J., (2005) "Failure Mechanisms of Polymer-Reinforced Concrete Masonry Walls Subjected to Blast," *Journal of Structural Engineering*, Vol. 131, No. 8, pp. 1194-1205.
7. Hamoush, S., McGinley, M., Mlakar, P., Murray, K., (2001) "Out-of-Plane Strengthening of Masonry Walls with Reinforced Composites," *Journal of Composites for Construction*, Vol. 5, No. 3, pp. 139-145.
8. DTRA/TSWG Program, (1999), "Blast Mitigation for Structures, 199 Status report on the DTRA/TSWG Program", National Academy Press, Washington D.C., 1999.
9. Eamon, C.D., Baylot, J.D., and O'Daniel, J.L., (2004), "Modeling Concrete Masonry Walls Subjected to Explosive Loading," *Journal of Engineering Mechanics*, Vol. 130, No. 9, pp. 1098-1106.
10. Tan, P.J., Reid, S.R., Harrigan, J.J., Zou, Z., Li, S., (2005), "Dynamic compressive strength properties of aluminum foams. Part I—experimental data and observations," *Journal of the Mechanics and Physics of Solids*, No.53, pp. 2174–2205.
11. Gibson, L.J., and Ashby, M.F., (1988), "Cellular Solids – Structures and Properties," Progress Press, Oxford, England.
12. Guruprasad, S. and A. Mukherjee, (2000), "Layered sacrificial claddings under blast loading. Part II Experimental studies" *International Journal of Impact Engineering*, Vol. **24**: p. 975–984
13. Hanssen, A.G., L. Enstock, and M. Langseth, (2002) "Close range blast loading of aluminium foam panels" *International Journal of Impact Engineering*, Vol. **27** p. 593–618.

14. Hoff, G.C., (1971) "New Application for Low-Density Concretes," ACI SP 29-11, vol 29, pp. 181-220.
15. Bulson, P.S., "Buried Structures: Static and Dynamic Strength," Chapman and Hall Ltd., New York, NY, 1985.
16. Li Q.M. and Meng H., (2002), "Pressure-Impulse Diagram for Blast Loads Based on Dimensional Analysis and Single-Degree-of-Freedom Model," *Journal of Engineering Mechanics*, 128(1): 87–92.
17. Ma G.W., and Ye Z.Q., (2007), "Analysis of foam claddings for blast alleviation," *International Journal of Impact Engineering* 34 (2007) 60–70.
18. Ma G.W., and Ye Z.Q., (2007), "Effects of Foam Claddings for Structure Protection against Blast Loads," *Journal of Engineering Mechanics*, 133(1): 41-47.
19. Nian, W., Subramaniam, K.V., and Andreopoulos, Y., (2012), "Dynamic compaction of foam under blast loading considering fluid-structure interaction effects," *International Journal of Impact Engineering*, 50: 29-39.

TABLES AND FIGURES

Table 1: Parameters obtained from fitting Equation 1 to experimental data.

Density **kg/m^3** (lb/ft^3)	**E** **MPa** (psi)	**A**	ε_{po}	σ_{po} **MPa** (psi)	α
384 (24) [±4%]	**24** (3480) [±9%]	1/350 [±35%]	0.016 [±12%]	**0.384** (55.7) [±12%]	2.9 [10%]
480 (30) [±3%]	**35** (5076) [±5%]	1/250 [±25%]	0.018 [±6%]	**0.63** (91.4) [±6%]	2.8 [10%]

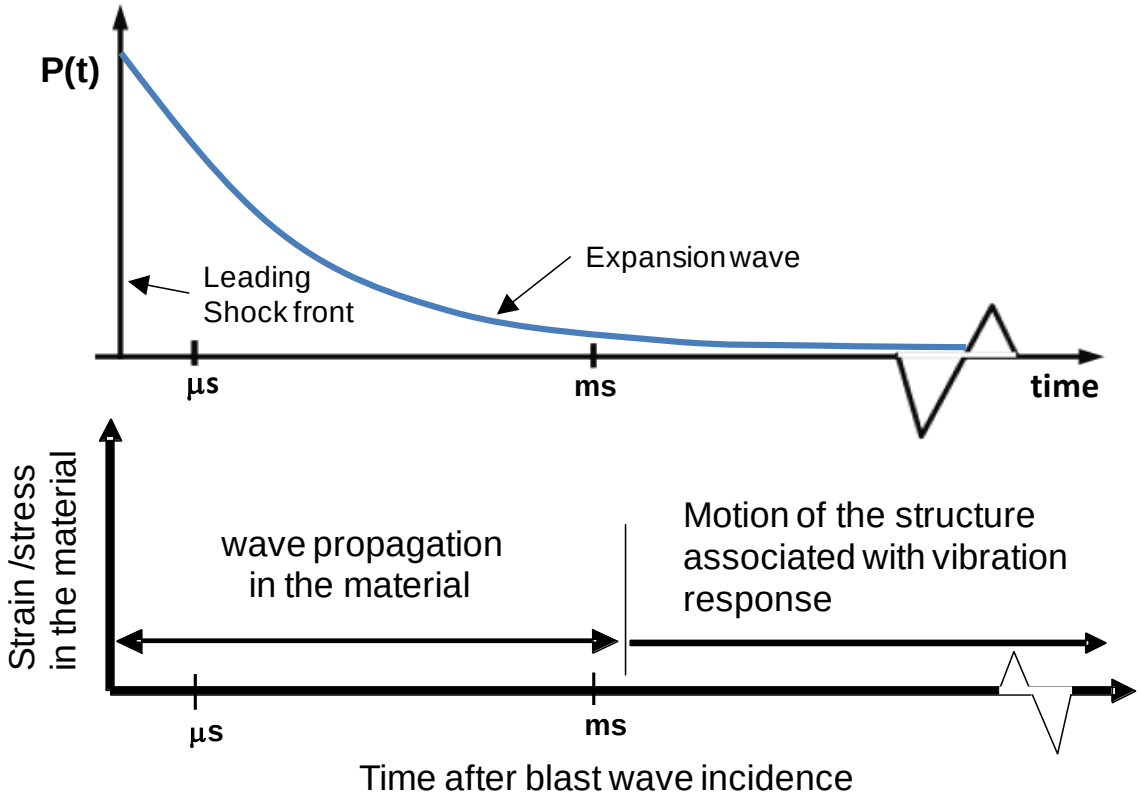

Fig. 1 – Schematic representation of blast pressure wave and the time scales associated with blast response.

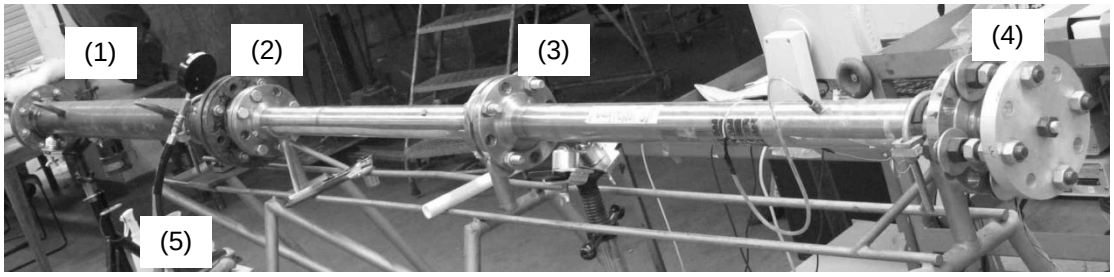

(a)

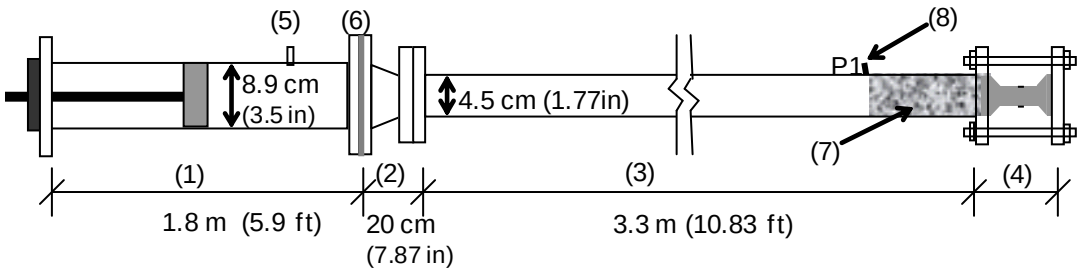

(b)

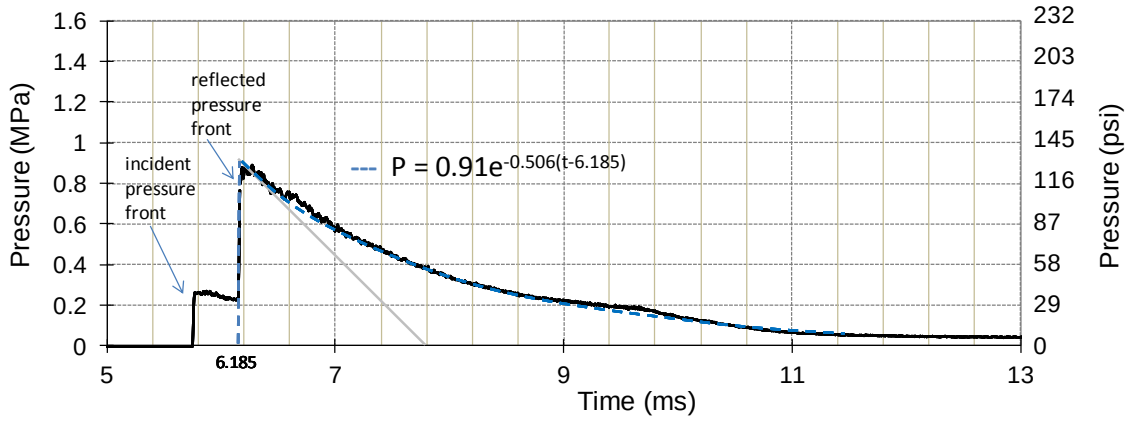

(c)

Fig. 2 – Shock tube test facility: (a) photograph and (b) schematic diagram. 1) driver section; 2) nozzle; 3) driven section; 4) instrumented step rod; 5) high-pressure gas inlet; 6) diaphragm; 7) specimen; 8) pressure transducer; (c) Typical pressure history measured at pressure transducer P1.

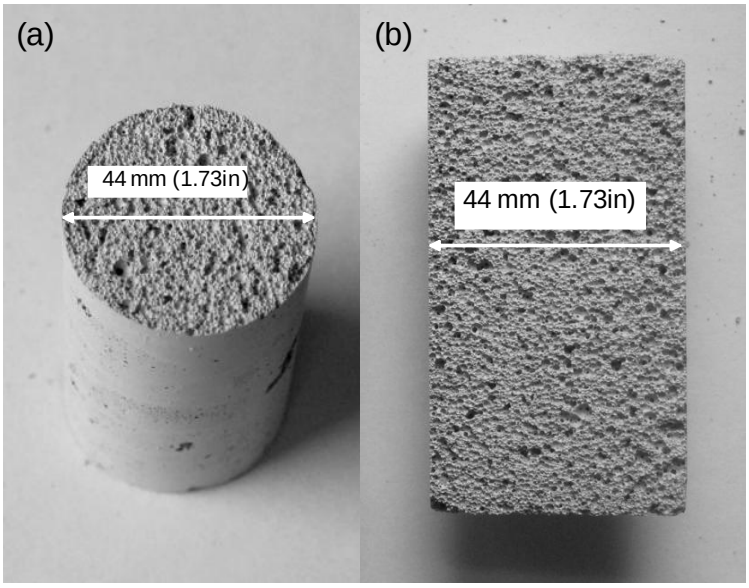

Fig. 3: Photographs of the cellular concrete sample (a) cross-section and (b) a section along longitudinal axis.

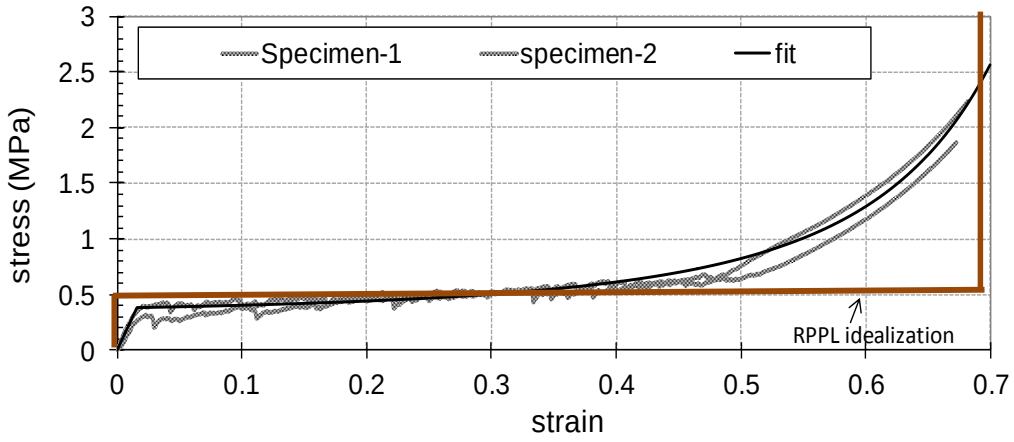

Fig.4 – Static stress-strain curves of cellular concrete.

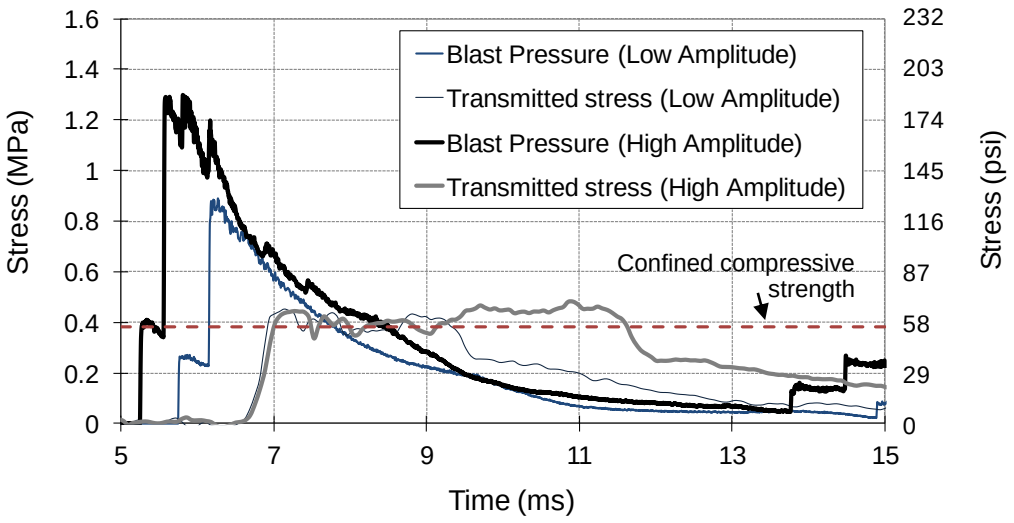

(a)

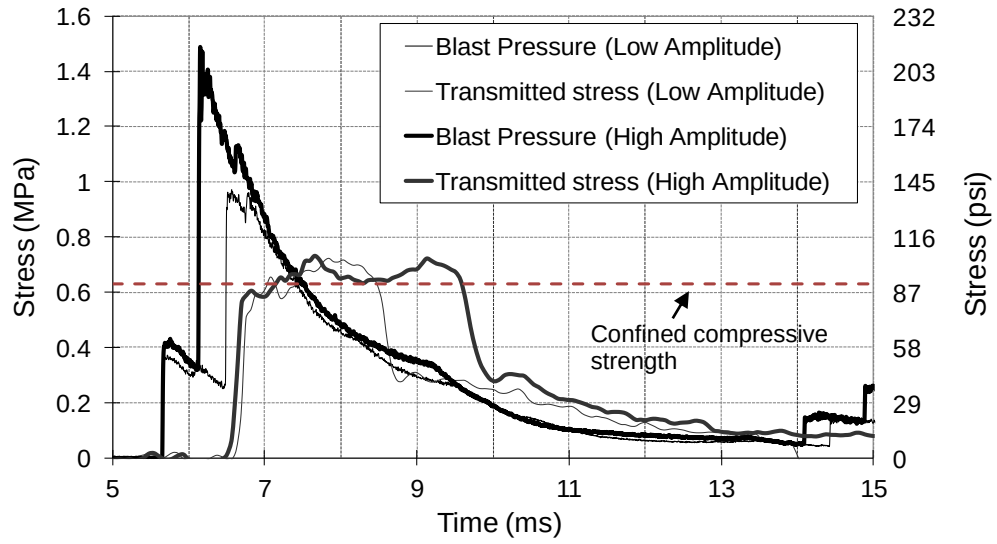

(b)

Fig. 5 – Applied blast pressure and transmitted stress histories for blast pressure loading with different amplitudes for cellular concrete with different crushing strength: (a) Dry density equal to 384 kg/m^3 and crushing strength equal to 0.384 MPa (55.7 psi); and (b) Dry density equal to 480 kg/m^3 and crushing strength equal to 0.63 MPa (91.4 psi).

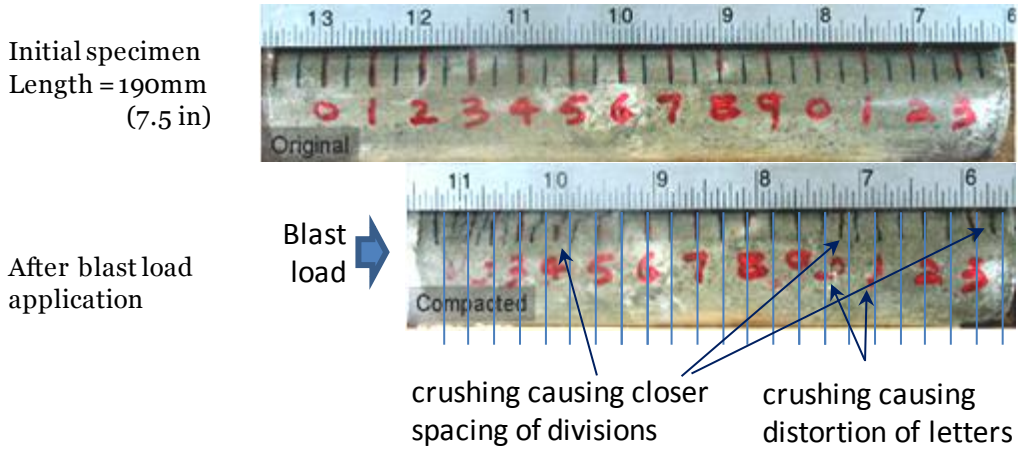

Fig. 6 – Photograph of cellular concrete specimens with initial length, L = 190 mm (7.5 in) and dry density equal to 384 kg/m^3: (a) before testing; and (b) after application of low amplitude blast.

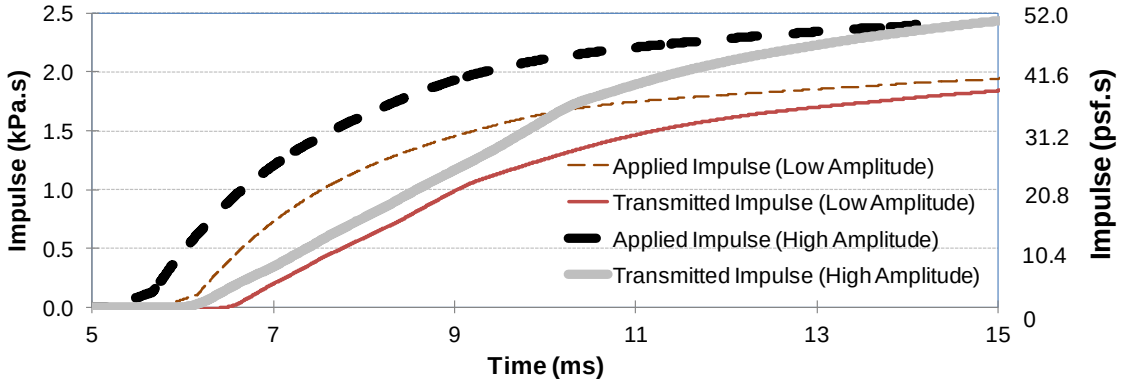

Fig. 7 – Impulse as a function of time for applied pressure loading and transmitted stress history.